

# Impact of Diaphragm Behavior on the Seismic Design of Low-Rise Steel Buildings

COLIN A. ROGERS and ROBERT TREMBLAY

---

## ABSTRACT

Modern building codes allow engineers to use reduced seismic loads in design provided that the seismic load resisting system (SLRS) of the structure is adequately designed and detailed to withstand strong ground shaking through ductile inelastic response. This approach has been adopted by the North American model codes, which typically include special provisions to achieve satisfactory inelastic seismic performance. Single-story buildings often incorporate a steel roof deck diaphragm that is relied on to transfer lateral loads to the vertical bracing bents. The vertical braces are usually selected as the energy dissipating fuse element, while the diaphragm and other elements in the SLRS should be designed such that their capacity exceeds the nominal resistance of the braces. Steel bracing members designed for compression inherently possess significant reserve strength when loaded in tension, which means that large brace tension loads must be considered in the design of the surrounding protected structural components. Capacity design seismic provisions have led to the need for much thicker roof deck panels and more closely spaced diaphragm connection patterns compared with past practice in Canada. This paper describes the current U.S. seismic design approach and provides examples as it is applied to single-story buildings and their diaphragms. An overview of the related aspects of an ongoing research project on the flexibility and ductility of the roof diaphragm in low-rise steel buildings is also included.

**Keywords:** diaphragms, seismic performance, low-rise steel buildings.

---

## INTRODUCTION

Single-story buildings often incorporate a steel roof deck diaphragm that is relied on to transfer lateral wind and seismic loads to the vertical bracing bents. Roof deck diaphragms in North America are commonly constructed of corrugated cold-formed steel panels that are connected to the underlying structure and to one another at side-laps. Standing seam roofs (SSRs) also incorporate a form of steel deck, although it is not rigidly attached to the supporting structure; therefore, SSRs do not provide the necessary diaphragm action for the purposes of this discussion. Design of roof deck diaphragms for in-plane shear forces can be carried out using the *SDI Diaphragm Design Manual* (Luttrell, 2004). The flexural capacity of the diaphragm can be developed through the use of continuous chord members (Figure 1a). Transfer of the horizontal forces to the vertical bracing bents relies on the action of the diaphragm collector elements (Figure 1a).

Diaphragms may also contribute to the overall dynamic properties and response of a building due to their in-plane flexural and shear flexibility.

North American model building codes (ASCE, 2005; NRCC, 2005) and steel design specifications (AISC, 2005a, 2005b; CSA, 2005) allow engineers to use reduced seismic loads in design provided that the seismic load resisting system (SLRS) of the structure is adequately designed and detailed to withstand strong ground shaking through ductile inelastic response. Building codes and standards include special provisions to achieve satisfactory inelastic seismic performance for the various SLRSs used in steel building construction (Tremblay, 2005). In particular, the design of the vertical structural system must be carried out with strict compliance to capacity design principles, i.e., the fuse elements of the SLRS are sized and detailed to dissipate seismic input energy through cyclic inelastic response, whereas the remaining elements should be provided with sufficient capacity to carry the maximum forces that are anticipated along the lateral load path.

The vertical braces of steel buildings are usually selected as the energy dissipating fuse element in the seismic load-resisting system, while the other elements in the SLRS are designed to have a capacity that is equal to or exceeds the expected strength of the braces. Figure 1b depicts the hierarchy of inelastic behavior in the elements located in the SLRS. When tension-compression bracing is used the steel bracing members designed for compression inherently

---

Colin A. Rogers, Associate Professor, Department of Civil Engineering and Applied Mechanics, McGill University, Montreal QC, H3A 2K6, Canada (corresponding author). E-mail: colin.rogers@mcgill.ca

Robert Tremblay, Professor, Group for Research in Structural Engineering, École Polytechnique, Montreal, QC, H3C 3A7, Canada. E-mail: robert.tremblay@polymtl.ca

---

possess significant reserve strength when loaded in tension, which means that large brace tension loads must be considered in the design of the surrounding protected structural components. In Canada the SLRS of single-story buildings includes the roof diaphragm as well as the other components in the vertical structural system. This design objective is clearly stated in the 2005 National Building Code of Canada (NBCC) (NRCC, 2005): “Diaphragms and their connections shall be designed so as not to yield.” (Article 4.1.8.15.1) and in CSA-S16 seismic provisions: “In capacity design ... diaphragms and collector elements are capable of transmitting the loads developed at each level to the vertical seismic-force-resisting system” (Clause 27.1.2). These seismic provisions have led to the need for much thicker roof deck panels and more closely spaced diaphragm connection patterns compared with past practice, especially in areas of high seismicity. Complying with these newly introduced design requirements has impacted significantly on the cost of steel building structures in Canada, making this system less attractive economically than in past years (Tremblay and Rogers, 2005). In contrast, no specific guidance is given by AISC (2005a, 2006) to prevent yielding or failure of roof diaphragms or beams acting as collectors or chords, and the designer must refer to ASCE 7 (2005) for the design forces. A capacity design requirement for the diaphragm to meet the expected yield strength of the braces in an ordinary or special concentrically braced frame (OCBF or SCBF) with  $R > 3$ , for example, does not exist.

This paper contains a description of the U.S. seismic design provisions for low-rise steel buildings, as well as a design example of a single-story building located in Boston, MA. The design is also performed assuming that the struc-

ture is located in Los Angeles, CA. In addition, the paper includes the interim findings of a study currently under way for which the objective is to develop seismic design strategies that account for the flexibility and ductility of the roof diaphragm in low-rise steel buildings. The scope of research includes quasi-static diaphragm shear tests (Tremblay et al., 2004; Essa et al., 2003), large-scale dynamic diaphragm tests (in progress), ambient vibration building measurements (Paultre et al., 2004; Lamarche, 2005; Tremblay et al. 2008a, 2008b), as well as dynamic analyses of representative buildings (in progress). At project end the aim is to make design recommendations on the following aspects: diaphragm stiffness under seismic loading, period of vibration for the building, seismic response modification factors, ductile detailing requirements and inelastic performance levels.

## SEISMIC DESIGN OF LOW-RISE BUILDINGS ACCORDING TO U.S. PROVISIONS

### Seismic Design Provisions

ASCE 7-05 provides the minimum seismic design loads for building structures in the U.S. Except for buildings with horizontal torsional irregularity, the equivalent lateral force procedure can be used for single-story steel buildings. This procedure comprises the application of an equivalent lateral seismic force that varies as function of the seismicity at the site, the soil type, the period of the buildings and the type of seismic load resisting system. The minimum lateral load, or seismic base shear,  $V$ , is given by:

$$V = C_s W \tag{1}$$

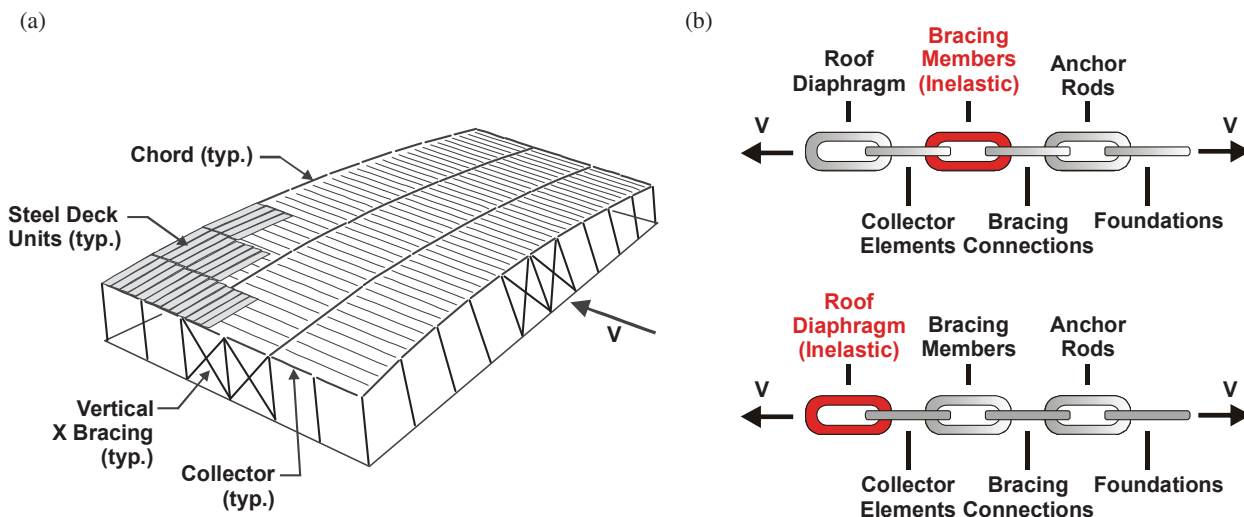


Fig. 1. Single-story buildings with capacity-based design concepts for SLRS.

where

$$\begin{aligned}
 C_s &= \frac{S_{DS}}{(R/I)} \\
 &\leq \frac{S_{D1}}{T(R/I)} \text{ for } T \leq T_L \\
 &\leq \frac{S_{D1}}{T^2(R/I)} \text{ for } T > T_L \\
 &\geq 0.044 S_{DS} I \\
 &\geq 0.01 \\
 &\geq \frac{0.5 S_1}{(R/I)} \text{ if } S_1 \geq 0.6g
 \end{aligned}$$

In these equations,  $W$  is the effective seismic weight,  $S_{DS}$  and  $S_{D1}$  are, respectively, the short-period and the one-second design spectral acceleration parameters,  $R$  is the response modification factor,  $I$  is the importance factor,  $T$  is the fundamental period of the building, and  $T_L$  is the long-period transition period at the site. For a single-story steel building,  $W$  includes the roof dead load, half the weight of the exterior walls, and 20% of the roof snow load when the snow load exceeds 30 psf. The spectral acceleration parameters are obtained from:

$$S_{DS} = \frac{2}{3} F_a S_s; S_{D1} = \frac{2}{3} F_v S_1 \quad (2)$$

where  $F_a$  and  $F_v$  are, respectively, the short-period and the long-period site coefficients that depend on the site class, and  $S_s$  and  $S_1$  are, respectively, the mapped spectral accelerations at short-period and one second corresponding to the maximum credible earthquake (MCE) level. Values of  $F_a$  and  $F_v$  are specified in ASCE 7 for different site classes, while values of  $S_s$  and  $S_1$  and  $T_L$  can be obtained from maps that are also included in ASCE 7. The period  $T$  for concentrically braced steel frames can be taken equal to the approximate period  $T_a = 0.02h^{0.75}$ , where  $h$  (ft) is the height of the building. Alternatively, the period obtained from dynamic analysis may be used, although the so-computed period cannot exceed the limit given by  $T = C_u T_a$ , where  $C_u$  is a coefficient that varies from 1.4 for high seismic zones to 1.7 for low seismic zones. The  $R$  factor depends on the type of lateral framing system. Single-story steel buildings typically rely on steel bracing for lateral resistance. Three categories of concentrically braced steel frames are described in ASCE 7: special concentrically braced steel frames (SCBFs); ordinary concentrically braced frames (OCBFs); and braced frames not specifically designed for seismic resistance. The main difference between the three systems is their expected inelastic deformation capacity under seismic ground motions. The AISC seismic design provisions (AISC, 2005a) provide detailing rules to ensure ductile inelastic response for the first two systems. More stringent requirements are prescribed for

SCBFs, which allow this framing system to qualify for an  $R$  factor of 6.0. An OCBF may be designed with less restrictive provisions; however, the seismic loads must be computed with  $R = 3.25$ . The third system, for which special ductility detailing requirements need not be considered, must be designed with  $R = 3.0$  according to the AISC specification (AISC, 2005b). The importance factor varies from 1.0 to 1.5, depending upon the occupancy category.

Also of key importance in seismic design is the Seismic Design Category of the building. This parameter depends on the occupancy category and the spectral acceleration values at the site. Seismic Design Categories A and B typically apply to buildings that are located in low seismic areas or represent a low hazard to human life in the event of failure. Braced steel frames designed with an  $R = 3.0$  are only permitted for seismic design categories A through C. Structures built in moderately or highly active seismic regions and/or buildings that represent a high hazard to human life or that are used for essential facilities generally are assigned to the more severe Seismic Design Category D. Where  $S_1 \geq 0.75$ , the structure is assigned to Seismic Design Category E, except that essential facilities are assigned to Seismic Design Category F. The OCBF system is limited to a height of 35 ft for Seismic Design Category D or E and is not permitted for Seismic Design Category F. The height limits for SCBFs—160 ft for Seismic Design Category D or E and 100 ft for Seismic Design Category F—typically would not apply to most single-story building applications. In ASCE 7, the seismic loads must be amplified by a redundancy factor,  $\rho = 1.3$ , for Seismic Design Category D, E or F. For braced steel frames, however, this factor can be taken equal to 1.0 if removal of one brace does not result in more than a 33% reduction in lateral strength nor result in an extreme torsional irregularity condition. The redundancy factor can also be ignored for rectangular buildings that are regular in plan provided that at least two bracing bays are constructed on each of the perimeter walls.

In view of their higher  $R$  factor, SCBFs are expected to develop significant inelastic response under the design earthquake. The aim of the AISC seismic provisions is to limit, for the most part, the inelastic demand to the bracing members so that the integrity of the gravity supporting system formed by the beams and columns will remain intact during a strong earthquake. Tension/compression bracing must be used for SCBFs. In addition, limits are imposed on the brace overall slenderness and width-to-thickness ratios to ensure ductile brace response and minimum energy dissipation without premature fracture under inelastic reversed cyclic loading. Brace connections must be designed to resist loads corresponding to the expected brace axial strength in tension,  $T_{exp} = AR_y F_y$ , and compression,  $P_{exp} = 1.1R_y P_n$ , where  $A$  is the brace cross-section,  $R_y$  is the ratio of the expected yield stress to the nominal yield stress,  $F_y$ , and  $P_n$  is the nominal brace

compressive strength. When the stress ratio,  $P_u/\phi_c P_n$ , under seismic load combinations exceeds 0.40, columns in bracing bents must be designed for the axial load obtained using the seismic load combinations, including system overstrength. Seismic load effects are amplified by the overstrength factor,  $\Omega_0$ , to approximate the maximum seismic induced force the columns will experience during strong ground shaking. In ASCE 7,  $\Omega_0 = 2.0$  for braced steel frames. These amplified seismic loads need not exceed the forces arising from  $1.1R_y$  times the nominal strengths of the connected braces nor the forces producing uplift of the foundation.

OCBFs are expected to undergo limited inelastic deformations under a design earthquake; thus fewer, less stringent ductility requirements apply. Both tension/compression and tension/only bracing designs are permitted in this category. The braces must still meet limits on their slenderness and width-to-thickness ratios. Brace connections must have a tensile strength equal to or greater than the expected brace yield tensile strength,  $T_{exp} = AR_y F_y$ , but need not exceed the load combination effects based upon the amplified seismic loads.

No specific guidance is given in AISC to prevent yielding or failure of roof diaphragms or beams acting as collectors or chords, and the designer must refer to ASCE 7 for the design forces for these components. For single-story structures, roof diaphragms are designed for the lateral force  $V$ , but this force must not be less than  $0.2S_{DS}IW$  and need not exceed  $0.4S_{DS}IW$ . The redundancy factor,  $\rho$ , must be the same as that used for the vertical bracing bents. Collector beams must be capable of transferring the forces used in the design of the diaphragm to the supporting framework. For Seismic Design Category C, D, E or F, the collector elements must resist the load combinations including seismic loads amplified for overstrength. No specific requirement is given for beams acting as diaphragm chords and it is assumed that forces consistent with diaphragm design can be used.

In the analysis of a building's structure, the minimum accidental eccentricity corresponding to 5% of the dimension perpendicular to the loading direction must be considered if the diaphragm is anticipated to act as a rigid element. Resistance to the induced in-plane torsional moments can be assumed to be provided by all bracing bents if the roof diaphragm has sufficient in-plane stiffness to efficiently distribute the loads to the vertical system. If the diaphragm is flexible, the load becomes essentially resisted only by the bracing bents acting in the direction parallel to the applied load. Single-story buildings are said to have a flexible diaphragm when the maximum in-plane deformation of the roof diaphragm is more than twice the average of the building deflections computed along the two end walls parallel to the direction under consideration. ASCE 7 requires that in-plane deformations of the roof diaphragm be included in the determination of the building story drift. In this calcu-

lation, the deformations from elastic analysis,  $\delta_{xe}$ , must be multiplied by  $C_d/I$  to obtain the design story drift reflecting inelastic response,  $\Delta$ . The factor  $C_d$  is, respectively, equal to 5.0 and 3.25 for SCBFs and OCBFs. For braced steel frames designed without ductile detailing,  $C_d = 3.0$ . When checking drift limits, it is noted that ASCE 7 allows the use of deflections due to seismic loads based on the building fundamental period obtained from dynamic analysis, without applying the upper limit  $C_u T_a$ .

### Building Design Example (Boston)

The simple rectangular building located in Boston, MA, shown in Figure 2a is used to illustrate the seismic design provisions for single-story buildings with lateral seismic loads resisted by steel braced frames acting together with a metal roof deck diaphragm. The roof structure is made of open web steel joists supported on steel trusses spanning across the entire width of the building. Single-bay X-bracing is used on each of the four exterior walls. Only the design of the seismic load resisting system in the direction parallel to the short walls is considered in this example. In addition, the calculations are performed assuming that an SCBF system with  $R = 6.0$  and  $C_d = 5.0$  is adopted for the bracing bents. The main differences between this and an OCBF design are discussed at the end of the example.

The dead load of the roof and walls are given in the figure together with the roof snow load. The seismic weight,  $W$ , is equal to 593 kips. An Occupancy Category II is assumed for the building, the site class is D, and the importance factor  $I = 1.0$ . The seismic data  $S_s$ ,  $S_1$  and  $T_L$  for the chosen location are given in Figure 2a. For this site,  $F_a = 1.56$  and  $F_v = 2.4$ , which gives design spectral accelerations  $S_{DS} = 0.31g$  and  $S_{D1} = 0.11g$ . The building is 22 feet tall and the period  $T_a = 0.02(22)^{0.75} = 0.20$  s. For this site ( $S_{D1} = 0.11g$ ), the factor  $C_u = 1.6$  and the amplified period  $C_u T_a = 0.32$  s. This period estimate is used for the design and, hence, will need to be checked at the end of the design process. Using these parameters in Equation 1, it is found that  $C_s = 0.052$  and  $V = 30.8$  kips. Following ASCE 7 procedures, it is determined that the building can be assigned to Seismic Design Category B. Therefore, the redundancy factor,  $\rho$ , can be taken equal to 1.0.

The bracing bents are designed first. At this point, one cannot determine whether the roof diaphragm will be classified as flexible; as such it is conservatively assumed that the diaphragm is rigid and that in-plane torsional effects must be accounted for. The structure is symmetric and accidental torsion is included by moving the center of mass (CM) away from the center of rigidity (CR) by 5% of the length of the building (10 ft), as prescribed in ASCE 7 and illustrated in Figure 2b. Assuming that all four bracing bents are of equal stiffness, the load on the bracing bent on gridline A

is equal to 54%  $V = 16.6$  kips. This load is resisted equally by the tension and compression acting braces (Figure 2c). Once the braces and columns are designed, analysis of the braced frame will be performed to assess gravity load effects on the braces. At this step, a first trial is made using the compression force of 11.0 kips; square tubing HSS  $3 \times 3 \times 3/16$  conforming to ASTM A500 Grade C ( $F_y = 50$  ksi) is selected for the braces. The factored resistance of these braces  $\phi P_n = 13.9$  kips, assuming a brace effective length  $KL = (0.5)(400 \text{ in.}) = 200$  in. The braces have a design thickness  $t_d = 0.174$  in., a cross sectional area  $A = 1.89 \text{ in.}^2$ , and they meet the AISC limits for overall slenderness ( $KL/r = 175 < 200$ ) and width-to-thickness ratio ( $b/t = 14.2 < 15.4$ ). For steel tubing,  $R_y = 1.4$  in the AISC seismic provisions and the expected brace capacities can be determined:  $T_{exp} = 132$  kips and  $P_{exp} = 23.8$  kips.

W-shapes made of ASTM A992 steel ( $F_y = 50$  ksi) are used for the columns. Axial compression due to gravity roof dead and snow loads are, respectively, equal to  $P_D = 5.25$  kips and  $P_S = 8.75$  kips. Since the brace  $KL/r = 175$  exceeds  $4(E/F_y)^{0.5} = 96$  (taking  $E = 29,000$  ksi), the AISC *Seismic Provisions* require that the columns be designed to carry gravity load effects plus the brace force  $T_{exp}$  transferred to the column;  $P_E = 132[\sin(41.3^\circ)] = 87.1$  kips. A W8x40 shape is found adequate to withstand the various load combination effects and meet the minimum width-to-thickness limits prescribed for columns in the AISC *Seismic Provisions*. The analysis of the braced frame under combined gravity and seismic loads shows that the brace compression force is increased to 11.8 kips, still lower than the brace factored resistance (13.9 kips). The elastic deflection,  $\delta_B$ , of the bracing bent computed under half the seismic load (15.4 kips), is 0.11 in.

The roof diaphragm is formed of 1½-in.-deep, wide-rib (WR) Canam P3606 steel deck sheets having a trapezoidal cross-section. The sheets are 36 in. wide, with flutes spaced 6 in. on center, as illustrated in Figure 3a. The sheets are 25 ft long and span over four equal spans between the roof joists (see Figure 2a). No. 10 self-tapping screws are used for the side-lap connections whereas Hilti X-ENP-19 L15 pins are chosen to connect the steel deck to the supporting structure. The diaphragm design is performed according to the SDI method (Luttrell, 2004) together with the 2004 supplement to the 2001 specification for the design of cold-formed steel members (AISI, 2004). The resistance factor associated with fastener failure modes,  $\phi_{ds}$ , is equal to 0.65. In the direction studied the maximum shear flow in the diaphragm arises along gridline A with  $S_u = 16.6$  kips/100 ft = 0.166 kip/ft. A light diaphragm design consisting of 0.0295-in.-thick steel (22 ga.) panels is found adequate with two side-lap screws per joist span and pins installed on a 36/3 pattern (18 in. on center). Such a diaphragm has a factored shear resistance  $\phi_d S_n = 0.281$  kip/ft and a shear stiffness,  $G'$ , of 12.9 kip/in.

The edge beams along the 200-ft-long walls act as the chord members resisting the axial loads induced by the in-plane bending moment, which is produced by the seismic load of 30.8 kips assumed to be uniformly distributed over the length  $L = 200$  ft,  $w_E = 0.154$  kip/ft. The maximum axial loads develop at the diaphragm mid-span,  $P_u = (\pm 0.154)(200^2/8)/100 = \pm 7.7$  kips. This situation is illustrated in Figure 3b; W8x10 beams with a cross-sectional area,  $A = 2.96 \text{ in.}^2$ , are selected. It is noted that seismic loads acting parallel to the long walls also induce axial loads in the same beams and the worst scenario must be considered for the beam design. As illustrated in Figure 3c, when considering

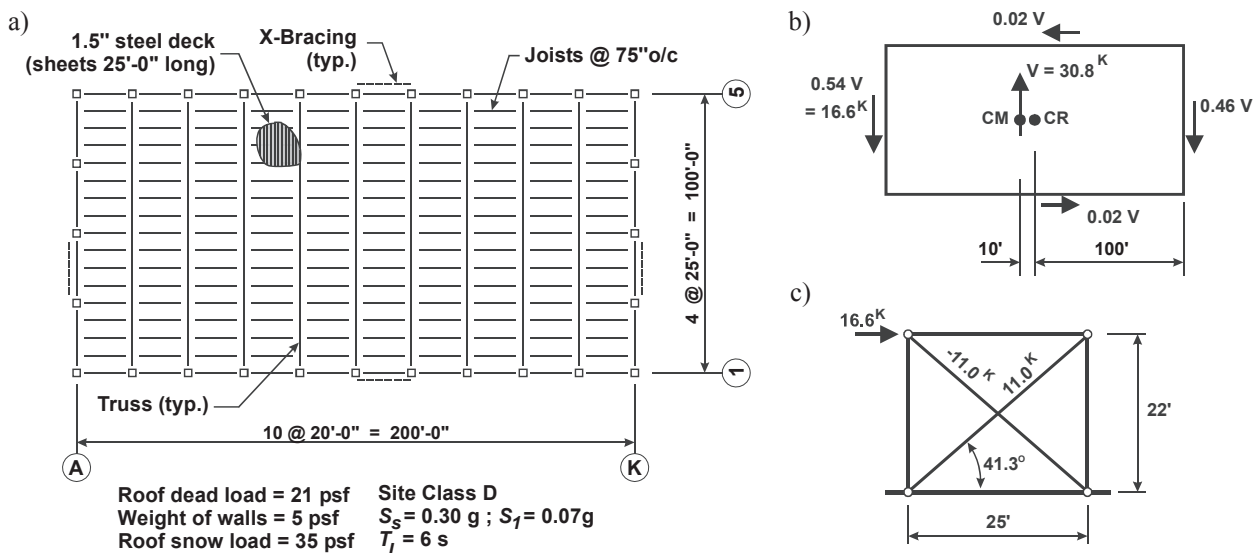


Fig. 2. (a) Plan view of the building studied, (b) in-plane torsion effects, and (c) bracing bent studied.

accidental eccentricity, a maximum force of 15.7 kips is transferred through the roof diaphragm to the bracing bent located along the long walls. The edge beams then act as collector elements transferring the shear flow from the diaphragm to the bracing bent (Figure 3d). In this particular case, the maximum compression axial load in the beams reaches 7.9 kips, which is more critical than the load induced when the same beams act as chord elements. It is noted that maximum forces in collector beams along braced column lines will be minimized if the bracing bents are located half-way along these grid lines. The designer must also provide proper connections between the steel deck and the perimeter members to allow the transfer of the shear flow from the diaphragm to the perimeter beams. In addition, attention must be paid to ensure the transfer of the computed beam axial loads through the beam-column joints. Once the diaphragm is designed and the chord members are selected, in-plane elastic deformations of the diaphragm due to flexure,  $\delta_F$ , and shear,  $\delta_w$ , can be determined. For this simple case, these two values can be calculated using:

$$\delta_D = \delta_F + \delta_w = \frac{5 w_E L^4}{384 E I_d} + \frac{w_E L^2}{8 G' b} \quad (3)$$

In this expression,  $I_d$  is the moment of inertia of the diaphragm in the direction considered ( $I_d = 2.13 \times 10^6 \text{ in.}^4$ ). The deflections  $\delta_F$  and  $\delta_w$  are, respectively, equal to 0.09 in. and 0.60 in., giving  $\delta_D = 0.69$  in. The ratio of the diaphragm

deflection to the bracing bent deflection (Figure 4a) is equal to  $0.69/0.11 = 6.3$ , which is much greater than 2.0, indicating that a flexible roof diaphragm could have been considered in design. The design should then be redone assuming that the diaphragm acts as a simply supported beam spanning between the bracing bents parallel to the load, thus neglecting the contribution of the bracing bents perpendicular to the load in the resistance to the in-plane torsion due to the accidental eccentricity of the seismic load. For regular rectangular buildings such as the one studied herein, a seismic force equal to  $0.55V$  would then need to be considered along each of the perimeter bracing bents. This is slightly larger than the values obtained assuming in-plane torsional resistance provided by four equally stiff bracing bents on the perimeter:  $0.54V$  and  $0.51V$ , in the short and long directions, respectively. For simplicity, however, the design obtained herein is kept unchanged in the example.

The design loads for earthquakes as calculated using ASCE 7 are based largely on the fundamental period of vibration of the vertical structure. It has, however, been shown through analytical means that the period of vibration of a single-story building with a flexible roof diaphragm may be longer than that predicted based on the stiffness of the vertical SLRS (Tremblay and Stierner, 1996; Medhekar, 1997; Tremblay et al., 2000). In the determination of the equivalent-static lateral loads for single story-buildings ASCE 41 (2006) allows for the introduction of the flexibility of the roof diaphragm to estimate the fundamental period of vibration.

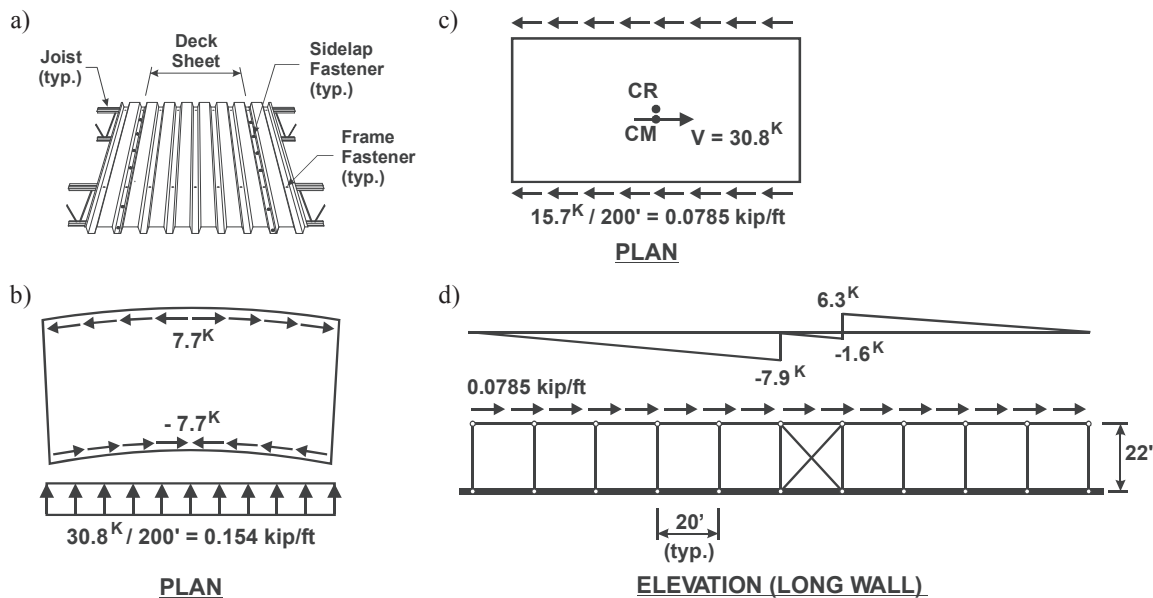


Fig. 3. (a) Steel deck panels, (b) axial loads in beams acting as diaphragm chord members, (c) force transfer from the diaphragm to the edge beam under seismic loads in the long direction, and (d) edge beams acting as collector elements under seismic loads acting in the long direction.

Similarly, an expression for the period was proposed by Medhekar (1997) and validated by shake table testing by Tremblay and Bérair (1999) and Tremblay et al. (2000). A longer building period can often provide for much lower seismic design forces based on the uniform hazard spectrum that is now required for design. Tremblay and Rogers (2005) illustrated that the use of this extended period of vibration can lead to significant savings in terms of the cost of the lateral load carrying system, mainly because of the lower design loads. Studies by Naman and Goodno (1986), Dubina et al. (1997), Tena-Colunga and Abrams (1996), Tremblay and Stierner (1996) and Tremblay et al. (2002), among others, also showed that the calculated seismic forces can be reduced by incorporating the diaphragm flexibility. Using the elastic deflections of the bracing bents and the diaphragm,  $\delta_B$  and  $\delta_D$  in Figure 4a, one can estimate the fundamental period of the structure with (ASCE 41, 2006):

$$T \approx \sqrt{\left(\frac{W}{V}\right)\left(0.10\delta_B + 0.078\delta_D\right)} \quad (4)$$

where  $\delta_B$  and  $\delta_D$  are in inches. When compared to the original equation found in ASCE 41, the ratio  $W/V$  has been incorporated in Equation 4 because the expression requires the use of deflections due to a horizontal load equal to the effective seismic weight,  $W$ . For the design presented herein, the computed fundamental period from Equation 4 is 1.12 s, which is much longer than the value assumed in design (0.32 s). For drift calculations, one uses the load obtained from

Equation 1 with this longer period, as permitted in ASCE 7-05. Figure 4b illustrates the significant reduction in design loads with  $V(T = 1.12 \text{ s}) = 0.0167W = 9.9 \text{ kips}$ , which is 32% of the seismic load determined using the period  $T = C_u T_a$ . Under this reduced lateral load, the elastic deflections  $\delta_B$  and  $\delta_D$  are respectively equal to 0.035 in. and 0.22 in. The design story drift can then be determined as  $\Delta = (5.0)(0.035 + 0.22)/1.0 = 1.28 \text{ in.}$ , giving an inter-story drift of 0.49%, which is less than the limit of 2% typically applicable to this type of building. One can check that for this structure P-delta effects are small and can be considered negligible.

In the structure as designed, the strength of the diaphragm is not related to the actual capacity of the vertical bracing system and there is no guarantee that the system will behave as intended under the design earthquake, i.e. with inelastic response developing in the bracing members that have been specially sized and detailed to undergo significant inelastic response without fracture. For instance, Figure 4c shows the diaphragm shear flow along the perimeter beams on the short exterior walls on grid lines A and F that was considered for the design of the roof diaphragm. The corresponding axial loads in the edge beams acting as collectors are also given in the figure (maximum = 8.30 kips). In Figure 4d, the same shear flow and beam axial loads are given when the braces reach their expected axial compression and tension strength  $P_{exp}$  and  $T_{exp}$  as determined earlier. The second set of forces is much greater, more than 7.0 times the forces used in design. However, considering that an  $R$  factor of 6.0 was used in the

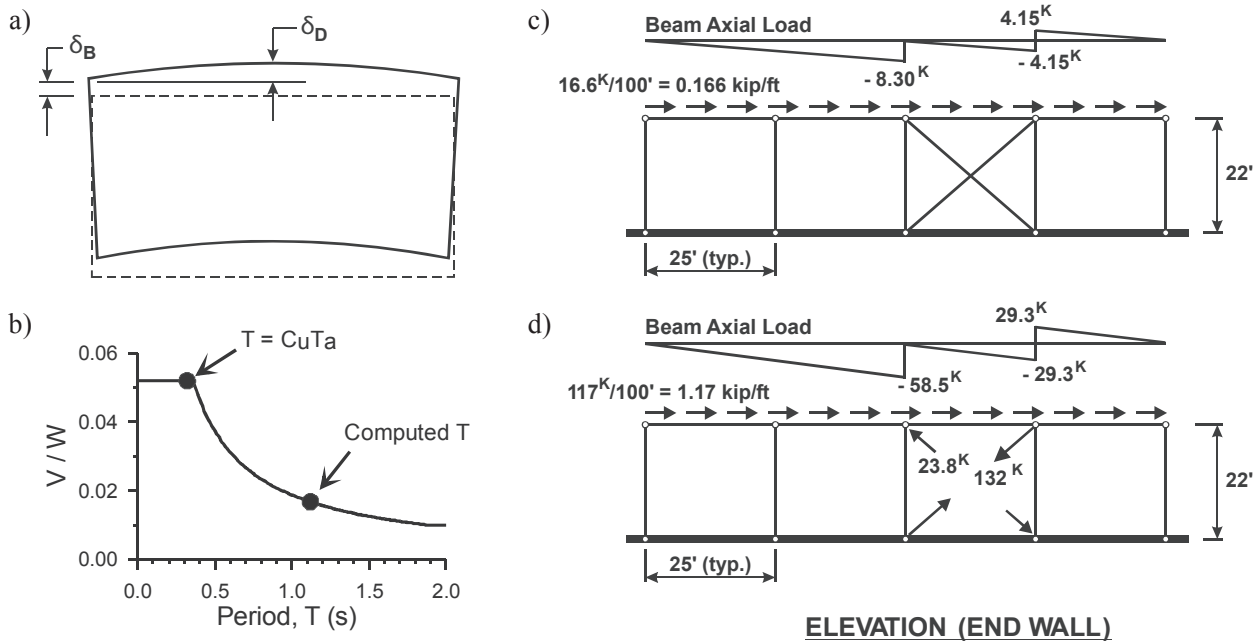


Fig. 4. (a) Bracing bent and roof diaphragm deformations, (b) variation of the seismic load with the period, (c) axial loads in edge beams acting as collector elements along the short walls under  $V = 30.8 \text{ kips}$ , and (d) axial loads in edge beams acting as collector elements along the short walls upon brace yielding.

**Table 1. Summary of the Design Parameters for the Building Examples**

Parameters	Boston area $S_s = 0.30, S_1 = 0.07, T_L = 6.0$ s SDC B $W = 593$ kips		Los Angeles area $S_s = 1.70, S_1 = 0.60, T_L = 12.0$ s SDC D $W = 453$ kips	
	SCBF	OCBF	SCBF	OCBF
$R$	6.0	3.25	6.0	3.25
$C_u T_a$ (s)	0.32	0.32	0.28	0.28
$V$ (kips)	30.8	56.9	85.6	158
$\rho$	1.0	1.0	1.0	1.3
Brace design	T/C	T/O	T/C	T/O
Brace section	HSS 3x3x $\frac{3}{16}$	L2 $\frac{1}{2}$ x2x $\frac{5}{16}$	HSS 4x4x $\frac{1}{4}$	2L3x3x $\frac{7}{16}$
$T_{exp}$ (kips)	132	71.3	236	262
$P_{exp}$ (kips)	23.8	—	75.1	37.5
$S_u$ (kip/ft)	0.166	0.307	0.462	1.11
Deck sheets	22 ga.	22 ga.	22 ga.	16 ga.
Frame fasteners	36/3	36/4	36/4	36/4
Screws/joist spacing	2	3	2	11
$G'$ (kips/in.)	12.4 (F)	22.8 (R)	25.1 (F)	102 (R)
$T$ from Eq. 4 (s)	1.12	1.11	0.71	0.56
$\delta/h_s$ (%)	0.49	0.53	1.67	1.43

Note: (F) = flexible diaphragm, (R) = rigid diaphragm

calculation of the design seismic load  $V$ , it is unlikely that such a high force demand will develop during the design earthquake. The resistance of the foundation to overturning uplift can also limit the forces delivered to the bracing bent. AISC (2006) provides an example illustrating how foundation uplift can be included in this calculation. Nevertheless, it is highly probable that forces in excess of the capacity of the perimeter beams and the diaphragm as designed will be reached in future earthquakes, which may cause severe damage and, possibly, failure of the diaphragm structure and collapse of the roof gravity system that it laterally supports. Caution should therefore be exercised by designers in the selection of the diaphragm and its chords and collectors to ensure that proper response will be achieved.

As mentioned, the 2005 NBCC in Canada states that diaphragms must be designed not to yield. They must therefore be provided with sufficient strength to match the expected strength (actual capacity) of the vertical system. The design forces need not exceed, however, the forces corresponding to elastic response, i.e., forces determined with the seismic response modification coefficients equal to 1.0. Had this concept been applied to the example building, the required shear strength for the roof diaphragm would have been  $S_u = (6.0)(16.6 \text{ kips})/100 \text{ ft} = 1.0 \text{ kip/ft}$ . In this case, the diaphragm design would call for a much stronger configuration such as 0.0474-in.-thick (18 ga.) deck panels connected

along the side-lap with eight screws per joist spacing and pins arranged in a 36/5 pattern.

The example building could have been designed using tension-only (T/O) bracing of the OCBF category. The main differences between the SCBF and OCBF design solutions are summarized in Table 1. An  $R$  factor of 3.25 would have been considered for the OCBF design, leading to a base shear force  $V = 56.9$  kips. For this system, L2x2 $\frac{1}{2}$ x $\frac{5}{16}$  single-angle braces made of ASTM A36 steel ( $A = 1.32 \text{ in.}^2$ ,  $F_y = 36 \text{ ksi}$ ) would have represented an acceptable solution [ $\phi T_n = 42.8 \text{ kips} > 40.9 \text{ kips} = (0.54)(56.9/\cos(41.3^\circ))$ ]. The required shear resistance for the diaphragm, without consideration of capacity design, would have been equal to 0.307 kip/ft [(0.54)(56.9)/100]. Deck panels 0.0295-in.-thick (22 ga.) are found adequate with three side-lap screws per joist span and pins installed on a 36/4 pattern (12 in. on center). Such a diaphragm has a factored shear resistance  $\phi_a S_n = 0.315 \text{ kip/ft}$  and a shear stiffness,  $G'$ , of 22.8 kip/in. For angles,  $R_y = 1.5$  in AISC *Seismic Provisions* and the expected brace tensile strength  $T_{exp} = 71.3$  kips. Had capacity design principles been adopted, the design force for the diaphragm would have been equal to 0.535 kip/ft, as governed by tension yielding of the braces. This value is nearly half that required for the more ductile SCBF system. This difference is attributed to the fact that tension/compression bracing is required for SCBFs. The size of the braces is governed by



the compression capacity requirement; since the braces are generally long and slender due to the height of single-story structures they possess significant overstrength resulting from the large difference between tension and compression capacities. When applying capacity design principles, this large overstrength impacts on the forces that will be delivered to the components in the SLRS, which need to remain essentially elastic.

### Building Design Example (Los Angeles)

The example building is designed for the Los Angeles area assuming the same site class (D), Occupancy Category (II) and importance factor ( $I = 1.0$ ). Table 1 gives the key design parameters for the SCBF and OCBF designs. At this site,  $F_a = 1.0$  and  $F_v = 1.5$ , which result in design spectral accelerations  $S_{DS} = 1.13$  g and  $S_{D1} = 0.60$  g. In view of these higher design spectral accelerations, the building must be assigned to a more severe Seismic Design Category D. The  $C_u$  factor for the period is also limited to 1.4, giving a design period  $C_u T_a = 0.28$  s. There is no roof snow load in Los Angeles, thus the seismic weight  $W$  reduces to 453 kips. The base shear for the SCBF and OCBF categories are, respectively, equal to 85.6 kips and 158 kips. For the SCBF system, tension/compression brace design is selected and a redundancy factor  $\rho = 1.0$  can be used despite the more critical SDC because removal of one brace results in less than a 33% reduction in lateral strength, and an extreme torsional irregularity condition does not exist. This is not the case when a tension-only bracing system is adopted for the OCBF example;  $\rho = 1.3$  must be used for this design.

Rigid diaphragm behavior is assumed for the distribution of the lateral loads, and 0.54  $V$  is considered to be resisted along the bracing bent. The selected braces and brace expected tensile and compressive strengths are given in Table 1. The design shear flow for the diaphragm and the properties of the selected roof deck system are also given in Table 1. For the SCBF system ( $R = 6.0$ ), the  $S_u$  value is 0.456 kip/ft [(0.54)(85.6) kips/100 ft] and a 22 ga. (0.0295 in.) deck design with 36/4 frame fastener pattern and eight side-lap screws per joist span is selected:  $\phi_d S_n = 0.489$  kip/ft and  $G' = 25.1$  kips/in. For this structure, a shear flow of 2.34 kips/ft is associated with the braces reaching their expected tensile and compressive strengths. This is 5.1 times the design value, indicating that the system may not perform as intended when the building is subjected to strong seismic ground shaking. For the OCBF system ( $R = 3.25$ ),  $S_u = 1.11$  kips/ft [(1.3)(0.54) (158) kips/100 ft]. This higher force demand requires much heavier diaphragm design: 16 ga. (0.0598 in.) deck sheets with closely spaced side-lap fasteners. In this OCBF design, back-to-back angles were selected for the braces. Even if tension-only braces are assumed in design, this type of brace still possesses compressive strength that should be

considered in capacity design ( $P_{exp} = 37.5$  kips with  $KL/r = 221$ ). The expected shear flow when the braces reach their tensile and compressive strengths is therefore equal to 2.25 kips/ft, approximately twice the design value according to the current seismic provisions. Although less pronounced than the building designs for the Boston area, both the SCBF and OCBF systems in Los Angeles have computed fundamental periods longer than the values assumed in design.

### EFFECT OF DIAPHRAGM FLEXIBILITY ON BUILDING PERIOD OF VIBRATION

In theory, accounting for the in-plane flexibility of the roof diaphragm may lead to more economical design solutions for single-story steel buildings, as was illustrated in the design example. However, recent ambient vibration studies on buildings of this type at the University of British Columbia and the University of Sherbrooke have shown that the period of vibration may be shorter than that predicted by analytical means (Paultre et al., 2004; Lamarche, 2005). The possible stiffening effect of non-structural roofing components diminishes to some extent the period lengthening effect of the roof deck diaphragm (Yang, 2003; Mastrogiuseppe et al., 2008), but this stiffening effect was found to be limited and not large enough to explain the differences between field measurements and analytical predictions. One drawback to the previous ambient vibration tests is that the building periods were obtained from the measurements of small building movement caused by relatively calm wind conditions. It is believed that roof diaphragms exhibit a stiffer response under such low amplitude loading because of the inherent friction resistance of the deck connections and the partial prevention of shear deformations from warping of the deck sheets at their ends due to the overlapping of the adjoining sheets. This represents a stiffer condition compared to the single sheet case that was considered in the development of the Steel Deck Institute (SDI) stiffness equations (Luttrell, 2004), which could also contribute to the observed differences between field tests and predictions (Figure 5). In this figure, the periods computed using Equation 4 are compared to those obtained from an empirical expression proposed by Lamarche (2005) based on field test data. The values  $0.05h_n$  and  $0.025h_n$  (where  $h_n$  = building height in m) are the predictor equations for the period of vibration of a concentrically braced frame based on the 2005 NBCC.

A more recent investigation that compared the results of ambient vibration measurements of a 74,100 ft<sup>2</sup> (approximately 23 ft in height, 300 ft by 234 ft in plan) single-story commercial building located in Magog, Quebec, with a 3D SAP 2000 building model (Figure 6a) showed that to obtain the measured periods (Figure 6b) a rigidly connected frame structure with infinitely stiff braces and continuous diaphragm panels would need to be assumed instead of the more common pin

connections and standard three- to four-span deck panels as would normally be used (Tremblay et al., 2008a, 2008a b). Analysis of the building accounting for the in-plane flexibility of the diaphragm and using assumptions commonly made in practice regarding member end fixity, brace stiffness and panel lengths led to a period of vibration of 1.11 s, significantly longer than the 0.39 s that was measured. In comparison, the NBCC would require that the period  $T_a$  be a maximum of 0.35 s, i.e.  $T_a \leq 0.05 h_n$ , which is in line with the ambient vibration result. A question remains as to whether this NBCC defined period should be allowed to be increased based on dynamic analyses of building models.

Preliminary large-scale dynamic tests were carried out at École Polytechnique of Montreal in the summer of 2007 on three diaphragm test specimens approximately 24 ft by 69 ft in plan (Figure 7). The test specimens were constructed using the popular 0.0295-in.-thick (22 ga.) 1½-in.-deep wide-rib deck profile with flutes spaced 6 in. on center. Nail frame connections and screw side-lap connections were used throughout. The test specimens represent a large portion of a building's roof, including the roof structure and roof

mass. The frame was mounted on rockers and two 220-kip high-performance dynamic actuators were used to apply the load along both edges of the supporting steel frame, thus representing the ground motion forces being transmitted to the roof by the vertical braces or the walls at the diaphragm ends. The intent was to vibrate the diaphragm at increasing amplitudes to identify whether a decrease of the in-plane shear stiffness would occur and if so by what extent. Information of this nature could be used to determine whether the period expressions defined in model building codes could be modified to account for diaphragm behavior under earthquake induced vibrations. Furthermore, the impact of end panel overlaps on the in-plane stiffness was investigated by testing diaphragm specimens both with and without end-laps. A variety of dynamic tests ranging from low amplitude basic white noise vibrations and harmonic signals to inelastic loading signals were used. In the tests, the influence of the loading amplitude on the period was assessed through all of the above dynamic loading protocols (Tremblay et al. 2008b). The inelastic response of the different diaphragm designs was also examined.

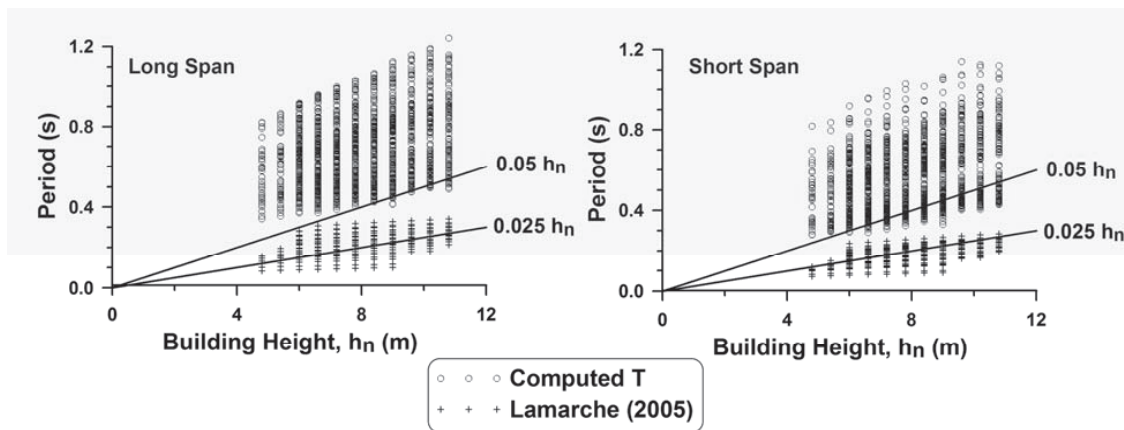


Fig. 5. Analytically computed periods and periods predicted using the empirical expression based on field test measurements (Tremblay and Rogers, 2005).

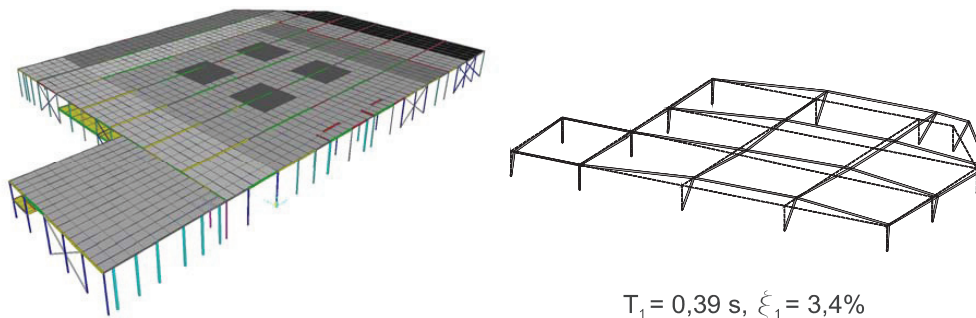


Fig. 6. (a) 3-D model of the structure and (b) measured fundamental mode and natural frequency (Tremblay et al., 2008a).

Figure 8 shows the variation of the fundamental period of vibration of a steel diaphragm specimen with the amplitude of dynamic excitation in terms of absolute acceleration at mid-span. Several white noise (random vibration signal with flat power spectral density used to obtain the frequency response) tests for which the displacement amplitude of the cycles was systematically increased were used to produce this figure. The plot shows that the period rapidly lengthens (flexibility increases) as the acceleration level exceeds that observed in field ambient vibration tests (typically less than 0.002 g). The higher initial stiffness is attributed to the lack of slip at the side-lap and deck-to-frame connections under low amplitude loading. Similarly, specimens submitted to a sine sweep protocol at increasing amplitudes showed that the resonant frequency of the diaphragm did not remain constant; rather the specimen became less stiff (resonant

frequency decreased) as larger amplitude cycles were applied. The results of the two loading protocols illustrate that the stiffness and natural frequency of a diaphragm are dependent on the level of deformation demand.

### DUCTILE DIAPHRAGM DESIGN AND BUILDING ANALYSES

It may also be possible to rely on the inelastic behavior of the diaphragm in design; that is, specify the roof deck diaphragm to be the fuse element in the SLRS instead of the vertical braces (Figure 1b). The shear capacity of the diaphragm can be adjusted by changing the connector spacing and panel thickness, thus leading to a capacity force that is only marginally higher than the code calculated seismic force. This could lead to a less expensive seismic load

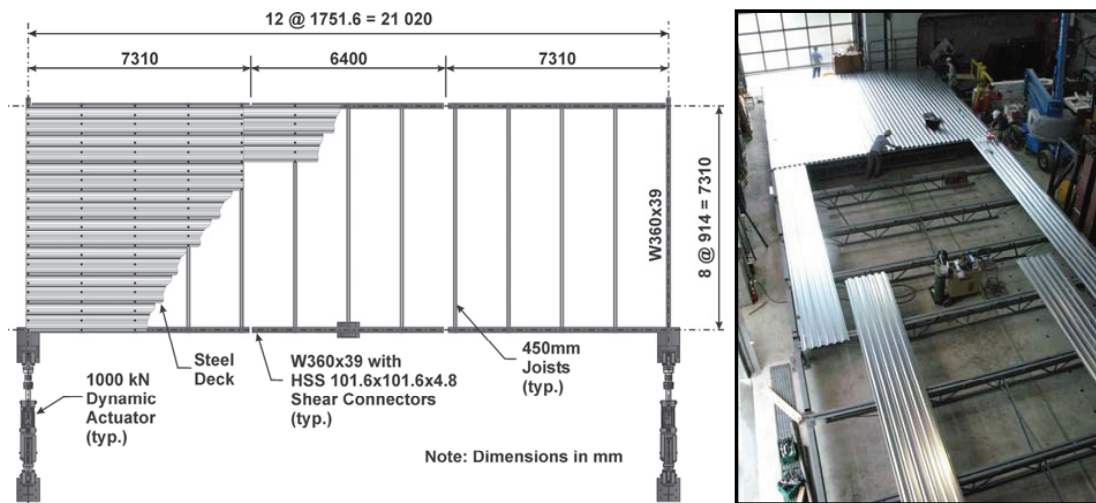


Fig. 7. Large-scale dynamic diaphragm test setup: (a) plan view and (b) during construction.

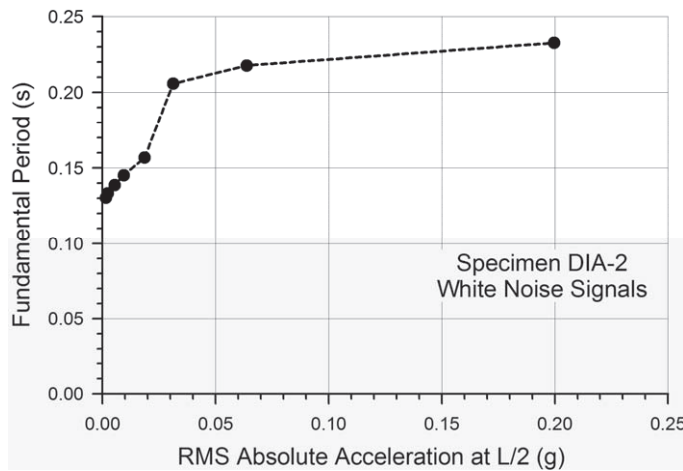


Fig. 8. Change in diaphragm period with white noise loading amplitude (adapted from Tremblay et al., 2008b).

resisting system and simpler detailing requirements for the braces and their connections because they would be expected to remain in the elastic range (Tremblay and Rogers, 2005). Experimental and analytical studies of the inelastic performance of diaphragms are summarized in the work of Tremblay et al. (2004) and Essa et al. (2003) (Figures 9 and 10). It was shown by means of testing that steel deck made of 0.0295-in.-thick (22 ga.) and 0.0358-in.-thick (20 ga.) sheets and connected with mechanical fasteners could undergo some limited cyclic inelastic deformations. It was noted, however, that relying on this inelastic behavior in the design of actual roof diaphragms could result in concentrations of large amplitude inelastic deformations in localized regions of the roofs, i.e., along braced wall lines, which could lead to undesirable diaphragm failures. This aspect could not be addressed in the past test programs due to the limited size of the diaphragm specimens (12 ft by 20 ft) and the type of displacement controlled loading that was used. Tests under dynamically applied loading on larger diaphragms were needed to properly assess the shear stiffness, distribution

of forces and inelastic deformations in metal roof deck diaphragms under actual seismic conditions, which lead to the tests illustrated in Figure 7.

The impact of capacity design provisions and period limitations on the seismic design of low-rise steel buildings was investigated (Tremblay and Rogers, 2005). Several design strategies were examined, including design without a capacity-based approach, capacity design with ductile bracing components, and capacity design assuming the cold-formed steel roof diaphragm acts as the main energy dissipation element in the SLRS. The effects of relaxing the period limitations and the capacity design forces for the roof diaphragm were also considered. A parametric study was carried out to evaluate the impact of the different strategies on the cost of the seismic load resisting systems (Figure 11). The building geometry, the seismic hazard level, the bracing configuration and the level of ductility were varied in this study. The results show that capacity design provisions have a significant impact on the structure, especially when tension-compression bracing is used. Substantial savings

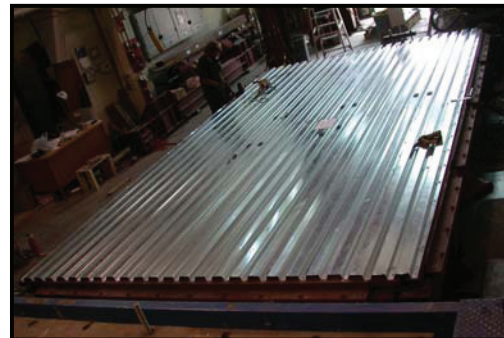
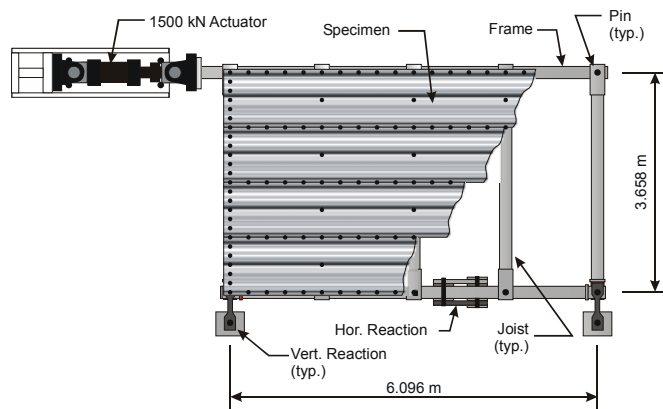


Fig. 9. Quasi-static diaphragm test specimen setup (Essa et al., 2003; Tremblay et al., 2004).

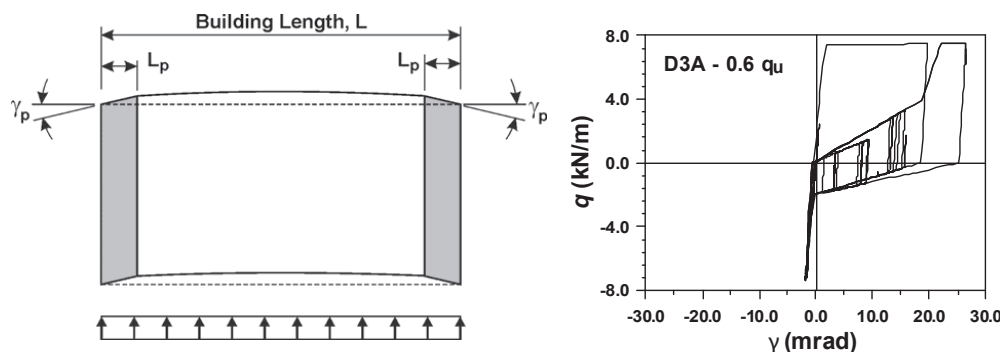


Fig. 10. Weak diaphragm design—concentration of inelastic design (adapted from Tremblay et al., 2004; Tremblay and Rogers, 2005).

could be realized with the use of a period obtained from methods of mechanics that incorporate diaphragm flexibility. Additional solutions for decreasing the cost of the structure also include relaxation of the capacity design provisions by reducing the upper limit on diaphragm forces or selecting the diaphragm as the main energy dissipating system. Nonlinear dynamic analyses of a limited number of these structures (Figure 12) were carried out using the RUAUMOKO (Carr, 2004) computer program. The roof diaphragm was modeled as a deep horizontal plane truss. A Stewart hysteretic model was selected for the diagonal roof truss members in order to reproduce the cyclic inelastic response measured for the screwed-nailed diaphragm system as described by Tremblay et al. (2004). The software and hysteretic model did not allow for the simulation of the strength degradation, which was observed during testing. The response of the example building was examined under one record from the 1994

Northridge earthquake scaled to match the design spectrum for Vancouver, Canada.

The time history response of the drift due to brace deformation ( $\delta_B$ ) and total building deformation ( $\delta_B + \delta_D$ ) for three design scenarios is provided in Figure 13: (a) protected diaphragm (brace fuse), where  $T_a = 0.05 h_n$ ; (b) weak (fuse) diaphragm, where  $T_a = 0.05 h_n$ ; and (c) weak (fuse) diaphragm, where  $T_a = T$  of the building accounting for the full diaphragm flexibility. Note: a protected diaphragm is selected so that its shear and flexural strength exceed the forces that correspond to the expected strength of the brace (fuse) elements; a weak diaphragm is selected to act as the inelastic fuse and thus has a strength that only needs to meet the building code seismic force. In all cases, the building experienced a maximum roof deformation that is below the prescribed limit of 2.5%  $h_r$ . A large portion of the overall story drift occurred in the bracing members due to

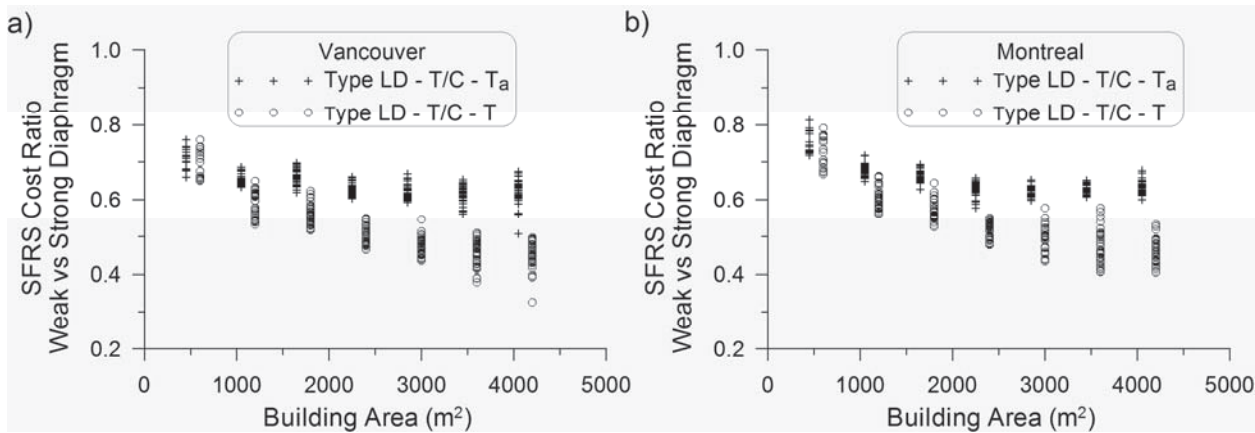


Fig. 11. SLRS cost ratios for (a) Vancouver and (b) Montreal (adapted from Tremblay & Rogers, 2005).

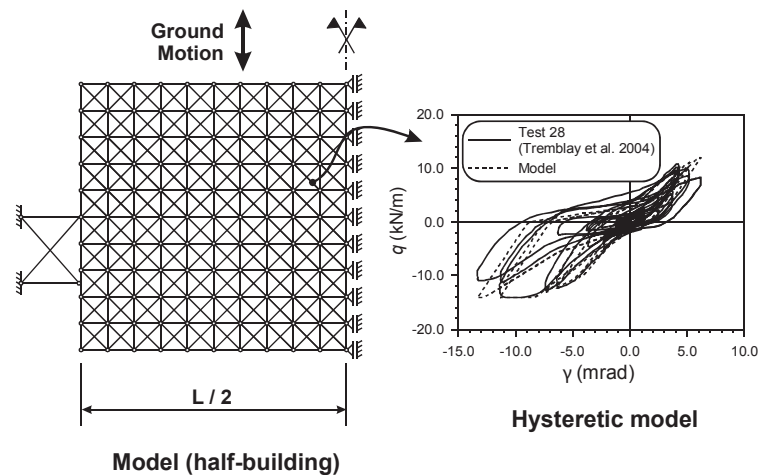


Fig. 12. Building model and Stewart hysteretic element (Tremblay and Rogers, 2005).

yielding; the in-plane diaphragm displacements were much less because this structural element was protected from entering into the inelastic range through implementation of the capacity design approach. After the strong motion segment of the record which ended at 14 s, significant deformations still developed in the bracing bents because the bracing members had been permanently elongated and were not able to offer any lateral resistance near the zero deformation position. As also expected from the design assumptions, plastic deformation was not observed in the roof diaphragm. In contrast, for the buildings in which the diaphragm was designed to be the fuse element, the peak roof displacement remained nearly the same but the inelastic demand switched from the bracing members to the roof diaphragm. The peak plastic demand in the roof,  $\gamma_p$ , is in accordance with the recommended permissible value of 10 mrad ( $= 10 \times 10^{-3}$  rad) of shear deformation for nailed-screwed decks (Essa et al., 2003).

It must be realized that this is a single example building subjected to only one ground motion and that the performance can vary significantly with ground motions and building dimensions. In particular, inelastic demand can be very sensitive to design and modeling assumptions, as well as loading conditions. In addition, this study was limited to uniform rectangular structures and it is expected that higher ductility demand can be induced in structures with irregularities or a non-symmetric footprint, as often encountered in practice. Nonetheless, the

results show that allowing the inelastic response of the structure to take place in the roof diaphragm made of thin steel sheets can result in an acceptable overall seismic performance. However, variation in strength and localized demand may result in excessive plastic deformations of the diaphragm, and further studies are needed before this design approach can be adopted.

## CONCLUSIONS

Seismic provisions of modern building codes now rely on capacity design procedures to provide a desired hierarchy of material yielding in the SLRS and better control of the inelastic response of a structure. For single-story steel buildings with concentrically braced steel frames, inelastic response is typically concentrated in the diagonal bracing members of the braced bays. Other components along the lateral load path, such as the roof diaphragm, including its chords and collectors, must be designed to resist the forces that will develop upon yielding in the vertical components of the seismic load resisting system. Current seismic provisions in the U.S. for buildings with  $R > 3$  do not result in entirely consistent design between the steel framing and the roof diaphragm. If full capacity design principles were required, much higher design forces would need to be applied to the diaphragm. For simple metal roof deck design, an SCBF example studied herein for the Boston area showed that the roof deck would need to be increased from a thickness of 0.0295 in. to 0.0474 in. (22 ga. to 18 ga.) with a more closely spaced fastener arrangement. Similar results were obtained for the other cases that were studied. Alternative design approaches that reduce the force demand on the diaphragm are being evaluated. The designer could possibly take advantage of the in-plane flexibility of the roof diaphragm, as this is currently permitted in ASCE 41 for the seismic retrofit of existing structures. Parametric studies performed for Canadian seismic conditions have shown that there is a significant potential for savings if the period from dynamic analysis is used in design. However, field ambient vibration test data seem not to support this approach and caution must be exercised before using the period prediction that accounts for roof diaphragm flexibility in seismic design. It may also be possible to allow for inelastic deformation in the roof diaphragm, instead of the diagonal bracing members. For thin deck sheets, these deformations can develop in the form of bearing or tearing in the vicinity of the deck fasteners. Deformation capacity is however limited and means must be taken to ensure that it will be properly distributed over the diaphragm area so that no concentration will develop that can lead to failure of the diaphragm system, i.e., a loss in the ability to transfer lateral forces to the bracing bents and a possible decrease in the effectiveness of the deck panels to laterally brace the supporting joist and beam structure. Research projects have been undertaken to examine the potential use of these two alternative design strategies.

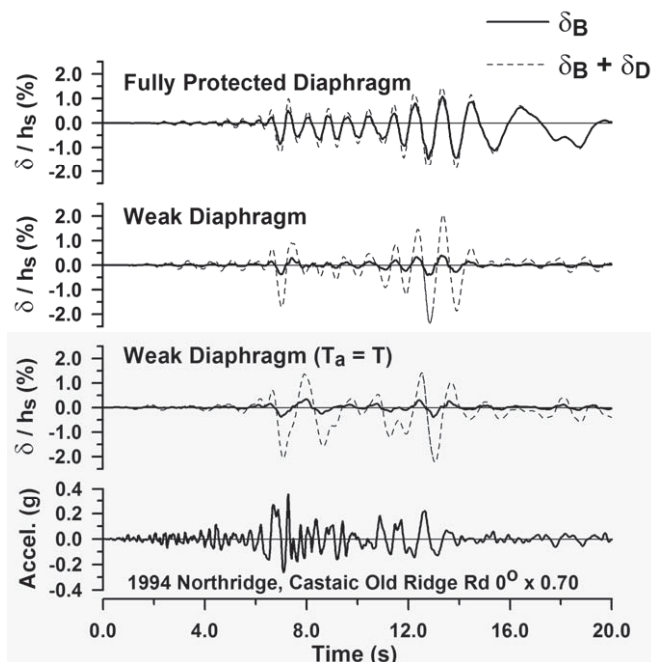


Fig. 13. Time histories of the story drifts for various design scenarios under a site-representative earthquake ground motion (adapted from Tremblay and Rogers, 2005).

## ACKNOWLEDGMENTS

The authors would like to acknowledge the support provided by the Canada Foundation for Innovation, the Canadian Sheet Steel Building Institute, the Canam Group Inc., WSB Consulting Structural Engineers, RJC Consulting Engineers, the Vancouver Steel Deck Diaphragm Committee, the Steel Deck Institute and Hilti Limited. Additional funding for this research was provided by the Natural Sciences and Engineering Research Council of Canada and the Funds for Research in Nature and Technologies of the Province of Quebec. The authors thank research assistants Camelia Nedisan, Charles-Philippe Lamarche, John Franquet and Robert Massarelli, as well as Patrice Belanger, technician at École Polytechnique, for their valuable assistance during the large-scale diaphragm test program.

## REFERENCES

- AISC (2005a), *Seismic Provisions for Structural Steel Buildings*, ANSI/AISC 341-05, American Institute of Steel Construction Inc., Chicago, IL.
- AISC (2005b), *Specification for Structural Steel Buildings*, ANSI/AISC 360-05, American Institute of Steel Construction Inc., Chicago, IL.
- AISC (2006), *Seismic Design Manual*, American Institute of Steel Construction Inc. and The Structural Steel Educational Council, Chicago, IL.
- ASCE 7 (2005), *Minimum Design Loads for Buildings and other Structures*, including Supplements Nos. 1 and 2, ASCE/SEI 7-05, American Society of Civil Engineers, Reston, VA.
- ASCE 41 (2006), *Seismic Rehabilitation of Existing Buildings*, American Society of Civil Engineers, Reston, VA.
- AISI (2004), *Supplement 2004 to the North American Specification for the Design of Cold-Formed Steel Structural Members*, 2001 ed., American Iron and Steel Institute, Washington, DC.
- Carr, A.J. (2004), RUAUMOKO, Inelastic Dynamic Analysis Program, Dept. of Civil Engineering, University of Canterbury, New Zealand.
- CSA (2005), *Supplement No. 1 to CAN/CSA-S16-01 Limit States Design of Steel Structures*, CSA-S16s1-05, Canadian Standard Association, Toronto, ON, Canada.
- Dubina, D., Zaharia, R. and Georgescu, M. (1997), "Stress Skin Design of Single-Story Steel Buildings in Seismic Areas," *Proceedings of the STESSA 97 Conference on the Behaviour of Steel Structures in Seismic Areas*, Kyoto, Japan, 1997, pp. 426–433.
- Essa, H.S., Tremblay, R. and Rogers, C.A. (2003), "Behavior of Roof Deck Diaphragms under Quasistatic Cyclic Loading," *Journal of Structural Engineering*, ASCE, Vol. 129, No. 12, pp. 1658–1666.
- Lamarche, C.-P. (2005), "Étude expérimentale du comportement dynamique des bâtiments de faible hauteur en acier," M.Sc.A. Thesis, Department of Civil Engineering, University of Sherbrooke, Sherbrooke, QC, Canada.
- Luttrell, L. (2004), *Diaphragm Design Manual*, 3rd ed., including Appendix VI Addendum November 2006, Publication No. DDMO3, Steel Deck Institute, Fox River Grove, IL.
- Mastrogiuseppe, S., Rogers, C.A., Nedisan, C.D. and Tremblay, R. (2008), "Influence of Non-structural Components on Roof Diaphragm Stiffness and Fundamental Periods of Single-Storey Steel Buildings," *Journal of Constructional Steel Research*, Vol. 64, No. 2, pp. 214–227.
- Medhekar, M.S. (1997), "Seismic Evaluation of Steel Buildings with Concentrically Braced Frames," Ph.D. Thesis, Department of Civil and Environmental Engineering, University of Alberta, Edmonton, AB, Canada.
- Naman, S.K. and Goodno, B.J. (1986), "Seismic Evaluation of a Low-Rise Steel Building," *Engineering Structures*, Vol. 8, No. 1, pp. 9–16.
- NRCC (2005), *National Building Code of Canada*, 12th ed., National Research Council of Canada, Ottawa, ON, Canada.
- Paultre, P., Proulx, J., Ventura, C., Tremblay, R., Rogers, C., Lamarche, C.-P. and Turek, M. (2004), "Experimental Investigation of Low-Rise Steel Buildings for Efficient Seismic Design," *Proceedings of the 13th World Conference on Earthquake Engineering*, Vancouver, BC, Canada, Paper No. 2919.
- Tena-Colunga, A. and Abrams, D.P. (1996), "Seismic Behavior of Structures with Flexible Diaphragms," *Journal of Structural Engineering*, ASCE, Vol. 122, pp. 439–445.
- Tremblay, R. (2005), "Canadian Seismic Design Provisions for Steel Structures," *Proceedings of the 2005 North American Steel Construction Conference*, Montreal, QC, Canada, AISC, Chicago, IL, 12 pp.
- Tremblay, R. and Stiemer, S.F. (1996), "Seismic Behavior of Single-Storey Steel Structures with Flexible Diaphragm," *Canadian Journal of Civil Engineering*, Vol. 23, pp. 49–62.
- Tremblay, R. and Bérair, T. (1999), "Shake Table Testing of Low-Rise Steel Buildings with Flexible Roof Diaphragms," *Proceedings of the 8th Canadian Conference on Earthquake Engineering*, Vancouver, BC, Canada, pp. 585–590.

- Tremblay, R., Bérair, T. and Filiatrault, A. (2000), "Experimental Behaviour of Low-Rise Steel Buildings with Flexible Roof Diaphragms," *Proceedings of the 12th World Conference on Earthquake Engineering*, Auckland, New Zealand, Paper No. 2567.
- Tremblay, R. and Rogers, C.A. (2005), "Impact of Capacity Design Provisions and Period Limitations on the Seismic Design of Low-Rise Steel Buildings," *International Journal of Steel Structures*, Vol. 5, No. 1, pp. 1–22.
- Tremblay, R., Rogers, C.A. and Nedisan, C. (2002), "Use of Uniform Hazard Spectrum and Computed Period in the Seismic Design of Single-Storey Steel Structures," 7th U.S. National Conference on Earthquake Engineering, Boston, MA, Paper No. 195.
- Tremblay, R., Rogers, C., Martin, É. and Yang, W. (2004), "Analysis, Testing and Design of Steel Roof Deck Diaphragms for Ductile Earthquake Resistance," *Journal of Earthquake Engineering*, Vol. 8, No. 5, pp. 775–816.
- Tremblay, R., Nedisan, C., Lamarche, C.-P. and Rogers, C.A. (2008a), "Periods of Vibration of a Low-Rise Building with a Flexible Steel Roof Deck Diaphragm," 5th International Conference on Thin-Walled Structures, Brisbane, Australia, pp. 615–622.
- Tremblay, R., Rogers, C.A., Lamarche, C.-P., Nedisan, C.D., Franquet, J., Massarelli, R. and Shrestha, K.M. (2008b), "Dynamic Seismic Testing of Large Size Steel Deck Diaphragms for Low-Rise Building Applications," 14th World Conference on Earthquake Engineering, Beijing, China, Paper No. 05-05-0066.
- Yang, W. (2003), "Inelastic Seismic Response of Steel Roof Deck Diaphragms Including Effects of Non-Structural Components and End Laps," M.A.Sc. Thesis, Department of Civil, Geological and Mining Engineering, École Polytechnique, Montreal, QC, Canada.

